

# PLOS ONE

## ALFA - Airborne LiDAR Field-plot Analysis. Fast automatic point-cloud filtering algorithm for analysis of crop growth dynamics in field-plot experiments.

--Manuscript Draft--

<b>Manuscript Number:</b>	PONE-D-23-28678
<b>Article Type:</b>	Research Article
<b>Full Title:</b>	ALFA - Airborne LiDAR Field-plot Analysis. Fast automatic point-cloud filtering algorithm for analysis of crop growth dynamics in field-plot experiments.
<b>Short Title:</b>	ALFA - Airborne LiDAR Field-plot Analysis Algorithm
<b>Corresponding Author:</b>	Jan F. Humplik Palacký University in Olomouc Olomouc, CZECH REPUBLIC
<b>Keywords:</b>	crop height; plant growth dynamics; UAV LIDAR; point-cloud; Python; field-plot
<b>Abstract:</b>	Repeated measurements of crop height to observe plant growth dynamics in real field conditions represent a challenging task. Although there are ways to collect data using sensors on UAV systems, proper data processing and analysis are the key to reliable results. Here we present a fast algorithm ALFA for the processing of UAV LiDAR derived point-clouds to extract the information on crop height at many individual cereal field-plots at multiple time points. Seven scanning flights were performed over 3 blocks of experimental barley field plots between April and June 2021. Resulting point-clouds were processed by the new algorithm ALFA. The software converts point-cloud data into a digital image and extracts the traits of interest – the median crop height at individual field plots. The processing time was about 2 to 3 minutes on a standard PC for a single point-cloud of ca. 100 million points. Three different ways of crop-height data visualization are provided by the software to enable further analysis of the variability in growth parameters. ALFA software is a fast and reliable tool for extraction of plant height in individual field-plots that are often used in agricultural research or plant breeding. We offer this tool freely to the scientific community for non-commercial use.
<b>Order of Authors:</b>	Tadeáš Fryčák Tomáš Fürst, Dr. Radoslav Koprna, Dr. Zdeněk Špišek, Dr. Jakub Miřijovsky, Dr. Jan F. Humplík, Dr.
<b>Additional Information:</b>	
<b>Question</b>	<b>Response</b>
<b>Financial Disclosure</b>  Enter a financial disclosure statement that describes the sources of funding for the work included in this submission. Review the <a href="#">submission guidelines</a> for detailed requirements. View published research articles from <a href="#">PLOS ONE</a> for specific examples.  This statement is required for submission and <b>will appear in the published article</b> if	The work was supported by the ERDF project "Plants as a tool for sustainable global development" (No. CZ.02.1.01/0.0/0.0/16_019/0000827).

the submission is accepted. Please make sure it is accurate.

#### Unfunded studies

Enter: *The author(s) received no specific funding for this work.*

#### Funded studies

Enter a statement with the following details:

- Initials of the authors who received each award
- Grant numbers awarded to each author
- The full name of each funder
- URL of each funder website
- Did the sponsors or funders play any role in the study design, data collection and analysis, decision to publish, or preparation of the manuscript?
- **NO** - Include this sentence at the end of your statement: *The funders had no role in study design, data collection and analysis, decision to publish, or preparation of the manuscript.*
- **YES** - Specify the role(s) played.

\* typeset

#### Competing Interests

Use the instructions below to enter a competing interest statement for this submission. On behalf of all authors, disclose any [competing interests](#) that could be perceived to bias this work—acknowledging all financial support and any other relevant financial or non-financial competing interests.

This statement is **required** for submission and **will appear in the published article** if the submission is accepted. Please make sure it is accurate and that any funding sources listed in your Funding Information later in the submission form are also declared in your Financial Disclosure statement.

View published research articles from [PLOS ONE](#) for specific examples.

The authors have declared that no competing interests exist.

**NO authors have competing interests**

Enter: *The authors have declared that no competing interests exist.*

**Authors with competing interests**

Enter competing interest details beginning with this statement:

*I have read the journal's policy and the authors of this manuscript have the following competing interests: [insert competing interests here]*

\* typeset

**Ethics Statement**

N/A

Enter an ethics statement for this submission. This statement is required if the study involved:

- Human participants
- Human specimens or tissue
- Vertebrate animals or cephalopods
- Vertebrate embryos or tissues
- Field research

Write "N/A" if the submission does not require an ethics statement.

General guidance is provided below. Consult the [submission guidelines](#) for detailed instructions. **Make sure that all information entered here is included in the Methods section of the manuscript.**

**Format for specific study types**

**Human Subject Research (involving human participants and/or tissue)**

- Give the name of the institutional review board or ethics committee that approved the study
- Include the approval number and/or a statement indicating approval of this research
- Indicate the form of consent obtained (written/oral) or the reason that consent was not obtained (e.g. the data were analyzed anonymously)

**Animal Research (involving vertebrate animals, embryos or tissues)**

- Provide the name of the Institutional Animal Care and Use Committee (IACUC) or other relevant ethics board that reviewed the study protocol, and indicate whether they approved this research or granted a formal waiver of ethical approval
- Include an approval number if one was obtained
- If the study involved *non-human primates*, add *additional details* about animal welfare and steps taken to ameliorate suffering
- If anesthesia, euthanasia, or any kind of animal sacrifice is part of the study, include briefly which substances and/or methods were applied

**Field Research**

Include the following details if this study involves the collection of plant, animal, or other materials from a natural setting:

- Field permit number
- Name of the institution or relevant body that granted permission

**Data Availability**

Authors are required to make all data underlying the findings described fully available, without restriction, and from the time of publication. PLOS allows rare exceptions to address legal and ethical concerns. See the [PLOS Data Policy](#) and [FAQ](#) for detailed information.

Yes - all data are fully available without restriction

A Data Availability Statement describing where the data can be found is required at submission. Your answers to this question constitute the Data Availability Statement and **will be published in the article**, if accepted.

**Important:** Stating 'data available on request from the author' is not sufficient. If your data are only available upon request, select 'No' for the first question and explain your exceptional situation in the text box.

Do the authors confirm that all data underlying the findings described in their manuscript are fully available without restriction?

**Describe where the data may be found in full sentences. If you are copying our sample text, replace any instances of XXX with the appropriate details.**

- If the data are **held or will be held in a public repository**, include URLs, accession numbers or DOIs. If this information will only be available after acceptance, indicate this by ticking the box below. For example: *All XXX files are available from the XXX database (accession number(s) XXX, XXX).*
- If the data are all contained **within the manuscript and/or Supporting Information files**, enter the following: *All relevant data are within the manuscript and its Supporting Information files.*
- If neither of these applies but you are able to provide **details of access elsewhere**, with or without limitations, please do so. For example:

*Data cannot be shared publicly because of [XXX]. Data are available from the XXX Institutional Data Access / Ethics Committee (contact via XXX) for researchers who meet the criteria for access to confidential data.*

*The data underlying the results presented in the study are available from (include the name of the third party*

Software tool is freely accessible here: <https://github.com/frycaktadeas/alfa>  
The datasets analyzed during the current study are available from the corresponding author on reasonable request.

*and contact information or URL).*

- This text is appropriate if the data are owned by a third party and authors do not have permission to share the data.

\* typeset

Additional data availability information:

## 1 TITLE

2 ALFA - Airborne LiDAR Field-plot Analysis. Fast automatic point-cloud filtering algorithm for analysis of  
3 crop growth dynamics in field-plot experiments.

## 4 AUTHORS

5 Fryčák Tadeáš<sup>2</sup>, Fůrst Tomáš<sup>1</sup>, Koprna Radoslav<sup>2</sup>, Špíšek Zdeněk<sup>2</sup>, Miřijovský Jakub<sup>3</sup>, Humplík Jan F.<sup>2\*</sup>.

## 6 AFFILIATIONS

7 1 Department of Mathematical Analysis and Applications of Mathematics, Faculty of Science, Palacký  
8 University, 17. Listopadu 50, 771 46 Olomouc, Czech Republic.

9 2 Department of Chemical Biology, Faculty of Science, Palacký University, Šlechtitelů 27, 78371  
10 Olomouc, Czech Republic.

11 3 Department of Geoinformatics, Faculty of Science, Palacký University, 17. Listopadu 50, 771 46  
12 Olomouc, Czech Republic.

13 \*corresponding author ([jan.humplik@upol.cz](mailto:jan.humplik@upol.cz))

## 14 KEYWORDS

15 crop height; plant growth dynamics; UAV LIDAR; point-cloud; Python; field-plot

## 16 ABSTRACT

17 Repeated measurements of crop height to observe plant growth dynamics in real field conditions  
18 represent a challenging task. Although there are ways to collect data using sensors on UAV systems,  
19 proper data processing and analysis are the key to reliable results. Here we present a fast algorithm  
20 ALFA for the processing of UAV LiDAR derived point-clouds to extract the information on crop height  
21 at many individual cereal field-plots at multiple time points. Seven scanning flights were performed  
22 over 3 blocks of experimental barley field plots between April and June 2021. Resulting point-clouds  
23 were processed by the new algorithm ALFA. The software converts point-cloud data into a digital image  
24 and extracts the traits of interest – the median crop height at individual field plots. The processing time  
25 was about 2 to 3 minutes on a standard PC for a single point-cloud of ca. 100 million points. Three  
26 different ways of crop-height data visualization are provided by the software to enable further analysis

27 of the variability in growth parameters. ALFA software is a fast and reliable tool for extraction of plant  
28 height in individual field-plots that are often used in agricultural research or plant breeding. We offer  
29 this tool freely to the scientific community for non-commercial use.

## 30 INTRODUCTION

31 Intensity of plant growth provides key information about the plant's ability to withstand all possible  
32 life situations in various environments. Analysis of plant growth is especially useful when performing  
33 agricultural experiments and plant breeding programs. However, manual measurements are very  
34 laborious, and widely affected by inter-rater variability. Small field-plots that consist of a single  
35 treatment (genotype/variety) are often used as the basic unit in plant and agricultural research. To  
36 analyze growth (expressed as the change in the crop height in time), the crop height in individual field-  
37 plots is manually assessed by some "ruler" resulting in each unit (field-plot) being represented by a  
38 single number (or a few numbers). These numbers are taken to represent the crop height over the  
39 entire field-plot, regardless of possible spatial heterogeneity which is often observed in agricultural  
40 experiments. To obtain more reliable growth data, analysis of crop height in the entire plot area can  
41 be performed (Holman et al., 2016). This assures that variability in crop height formed by thousands  
42 of individual plants will be properly reflected in the results. Moreover, when plant growth is measured,  
43 several measurements of crop height are needed to cover most of the vegetative period. This  
44 advocates for automatic (e.g. UAV-aided) rather than manual approaches.

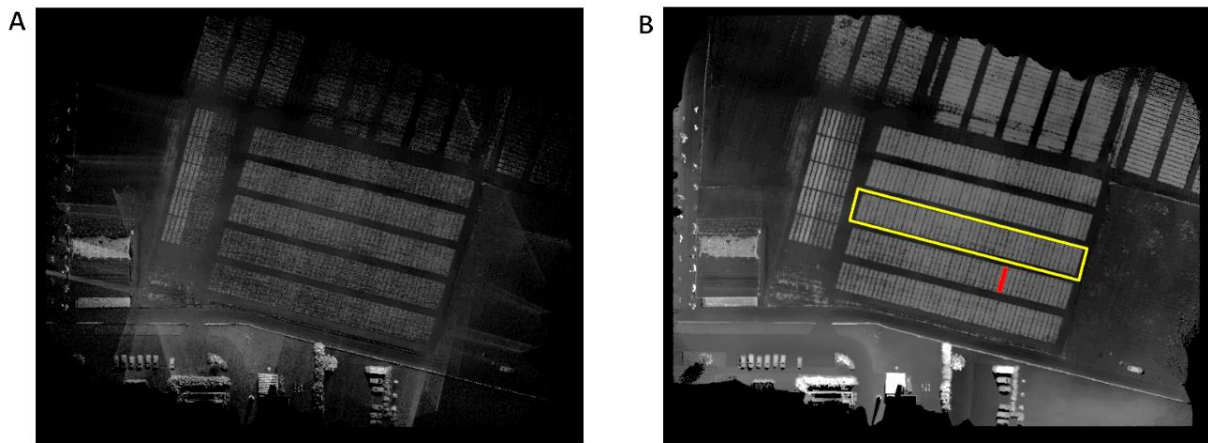
45 For these reasons, several remote-sensing approaches have been developed, such as structure-from-  
46 motion (SfM) or LiDAR-based solution. SfM techniques are cheaper but highly demanding from the  
47 data processing point of view. On the contrary, LiDAR systems are precise and can be analyzed  
48 relatively **fast however**, their price has limited their implementation so far (Iglhaut et al., 2019). LiDAR  
49 solutions are not limited to airborne systems only, they also include terrestrial LiDARs (Brede et al.,  
50 2017), **LiDARs on various moveable platforms such as tractors or sprayers** (French et al., 2016). Both  
51 SfM and LiDAR solutions are suitable for generation of crop height models (CHM) derived from point-

52 cloud files. The term CHM was invented for digital surface models (DSM) specifically applied to crops.  
53 CHM is defined as a normalized DSM (nDSM) which results from the subtraction of a digital elevation  
54 model (DEM = “ground” points only) from DSM containing other features, in our case plant canopy  
55 (Holman et al., 2016; Granshaw 2016).

56 It has been reported that crop-specific CHM perform better than generalized crop models (ten Harkel  
57 et al., 2019). Studies were focused on segmentation of individual plants as is typical for maize (Gao et  
58 al., 2022; Wang et al., 2023) or on segmentation of entire field-trial plots in case of other cereals,  
59 sorghum or cotton (Hütt et al., 2022; Montzka et al., 2023; Malambo et al., 2018; Liu et al., 2020). The  
60 conversion of point-clouds to CHM can be done manually using software for digital terrain model  
61 processing (Malambo et al., 2018), but specialized algorithms have also been reported (Zhu et al.,  
62 2021). Although the CHM can be efficiently utilized for segmentation of trial field-plots, they have been  
63 found insufficient for individual plant segmentation (Koch et al., 2006). For these specific purposes  
64 other methods based on direct-point segmentation were developed (Li et al., 2012). Other approaches,  
65 such as regional growth (Jin et al., 2018) or voxel-space projection (Wang et al., 2008), utilize features  
66 of individual points from the point-cloud **as well** the spatial relations between the points. Gao et al.  
67 (2022) recently proposed a method combining RGB orthophoto to identify seed points in young  
68 seedlings of maize for their later segmentation from LiDAR point-cloud using fuzzy based C-means  
69 clustering analysis. Our previous algorithm (Polák et al., 2021) was based on direct-point analysis  
70 strategy to segment trial field-plots of winter wheat. However, direct-point analysis is highly  
71 demanding on computing time. This reduced the applicability of our previous algorithm in datasets  
72 containing multiple point-clouds. Thus, we propose a new software based on the CHM strategy. The  
73 proposed solution reduces the computation time for a 1GB sized point-cloud file from several hours to  
74 several minutes without compromising precision and accuracy. In contrast to the previous algorithm,  
75 it can be run efficiently on a standard PC or laptop. The aim of this contribution is to describe the  
76 algorithm and show its utility in real conditions.

77 **IMPLEMENTATION**

78 The drone data is presented as a 3D point-cloud format, which consists of a list of  $[x, y, z]$  coordinates  
79 representing the positions of the recorded points. First, we convert this format into a 2.5D digital image  
80 format, allowing for the utilization of fast digital image processing methods. However, this conversion  
81 results in a loss of information because in a digital image, a single  $z$ -value is associated with each  $[x, y]$   
82 coordinate. Nevertheless, for crop height measurement purposes, this transformation is suitable.  
83 Additionally, no measured  $z$ -values are deleted; instead, all  $z$ -values corresponding to the same  $[x, y]$   
84 coordinate are averaged as described below.



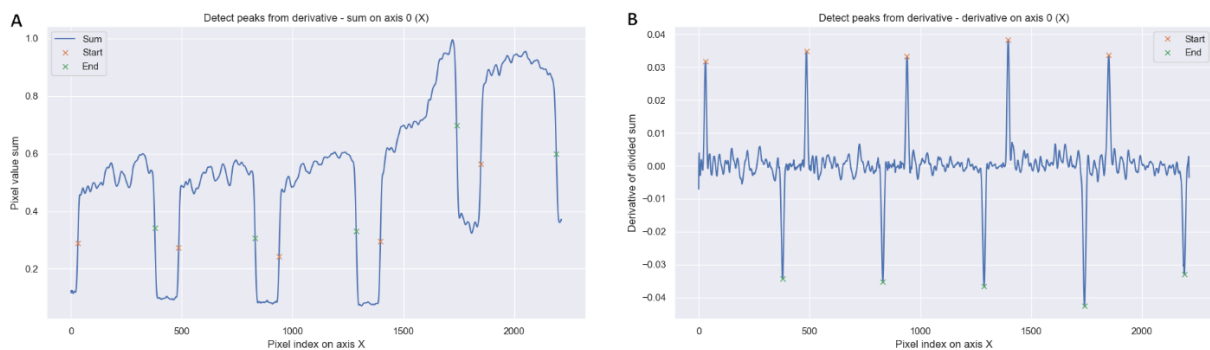
86 **Figure 1** Initial processing of the point-cloud data into the crop height model. A) The raw digital image obtained from the  
87 point-cloud data by averaging the  $z$ -values corresponding to the same  $[x, y]$  coordinate. B) The digital image after the  
88 application of the median filter to impute the missing values. A single *block* highlighted in yellow, a single *variant* within the  
89 block highlighted in red.

90 **Data filtering and rasterization** – The first step involves cleaning the point-cloud data by eliminating  
91 any outlier points that fall outside the 99.9% quantile in the  $x$ ,  $y$ , or  $z$  coordinates. Subsequently, a  
92 uniform rectangular grid is created in the  $x$ - $y$  plane, and each 3D point in the point cloud is assigned to  
93 the nearest grid pixel. The elevation of each grid pixel is then calculated as the average of all  $z$ -  
94 coordinates of cloud points assigned to that specific grid point. During this process, the elevation of  
95 certain grid points may remain undefined if no cloud points were assigned to them. To address this, a  
96 median filter is applied to impute the missing values. Furthermore, the  $z$ -coordinates are quantized to  
97 optimize the resulting image for a 16-bit depth. After completing these steps, the original 3D point-

98 cloud files are transformed and saved as significantly smaller 16-bit PNG images, while preserving the  
99 crop height information. Each PNG file corresponds to a specific drone measurement time. These PNG  
100 images can be conveniently processed using standard image processing tools.

101 **Selection of Region of Interest (ROI)** – The initial image from the repeated measurements undergoes  
102 rotation and cropping to a ROI, which is easily accomplished by the user through a Graphical User  
103 Interface (GUI). Next, all subsequent sequential images are automatically cropped to match the  
104 selected ROI, following the same process as the first image in the series.

105 **Instance segmentation algorithm** – Subsequently, the ROI undergoes segmentation to identify the  
106 individual field plots within the image for later CHM generation. Vertical and horizontal edges  
107 separating the field plots are automatically detected by summing the image values vertically and  
108 horizontally (Fig 2A). Peaks are automatically detected in the summed images by means of numerical  
109 derivatives (Fig 2B).



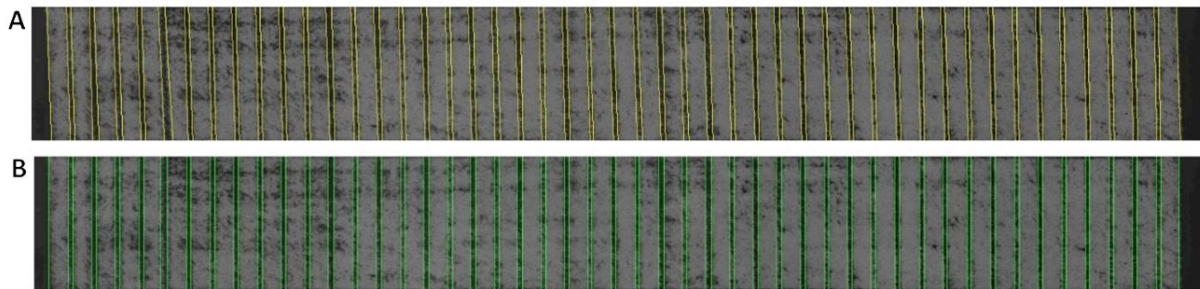
110

111 **Figure 2** Instance segmentation of individual fields. The digital image of a field block highlighted in yellow in Figure 1B is  
112 summed along the shorter edge. A) Vertical normalized sum of the processed image (blue) with automatically identified left  
113 (green) and right (orange) edges of the individual field plots. B) First derivative of the sum in panel A, enabling the automatic  
114 detection of the plot edges.

115

116 **Distortion correction** – The individual field plots are often thin and long and their images may be  
117 skewed. Thus, we apply a correction by fitting a parallelogram to the boundary of the field plots (Fig

118 3). The deformation is then automatically rectified through an affine transform algorithm, which is  
119 accessible within the OpenCV toolbox (OpenCV, 2008).



120

121 **Figure 3** Distortion correction A) A detail of a single *block* before the affine correction. B) The same *block* after the affine  
122 correction.

123 **Crop height computation** – The digital image is very “noisy” in the sense that z-values corresponding  
124 to neighboring grid points may be very different. To create a CHM, a maximum filter is used. Each pixel  
125 value in the image is substituted by the maximum of its neighbors. Intuitively, this operation  
126 corresponds to covering the original image by a deformable blanket. Next, the ground-surface (DEM)  
127 at time zero is subtracted from each image to account for any variability in the terrain. For each field-  
128 plot and each time of measurement, the following characteristics of the crop height are computed:  
129 mean, standard deviation, median, minimum, maximum, and several quantiles. The relative growth  
130 rate between time  $t_1$  and  $t_2$  is computed using the relation (Hoffmann and Poorter, n.d.)

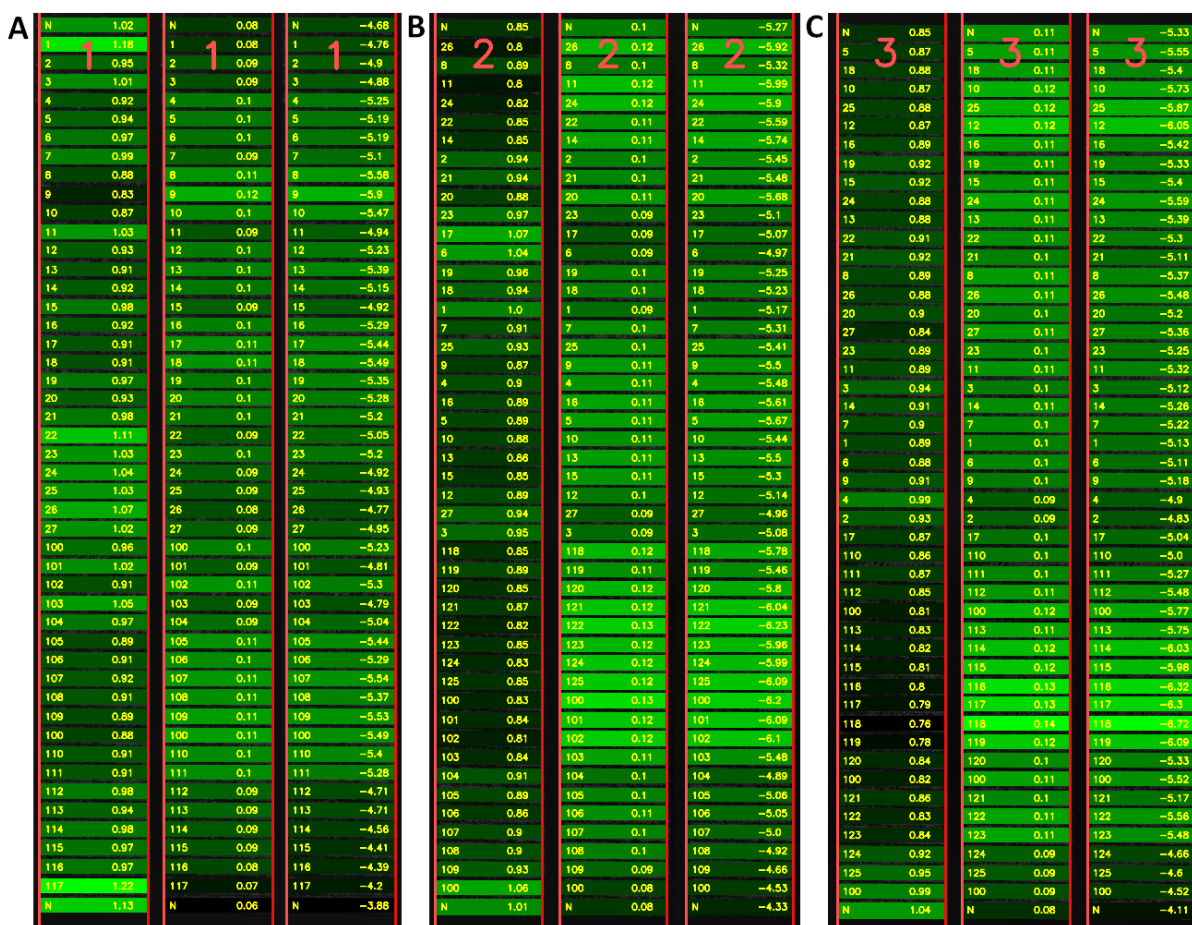
$$131 \quad RGR(t_1, t_2) = \frac{\ln S(t_2) - \ln S(t_1)}{t_2 - t_1}$$

132 Where  $S(t)$  is the median crop height at time  $t$ .

133 Each field plot is indexed by its *variant* number  $i$  and *block* number  $j$  (see Fig 1). The growth in each  
134 field-segment is analyzed as follows. Let  $S_{ij}(t)$  be the median crop height of variant  $i$  in block  $j$  at time  $t$ .  
135 A logistic growth curve is fitted to the data (separately in each field plot). The logistic curve is defined  
136 by:

$$137 \quad S(t) = \frac{A}{1 + \exp(-Bt - C)}$$

138 Where  $A$  characterizes the maximum height that the crop would reach if observed long enough,  $B$   
 139 captures the growth velocity, and  $C$  captures growth onset (for review see Tjørve, 2003). The  
 140 parameters  $A$ ,  $B$ ,  $C$  are found using a standard non-linear least squares regression (implemented in  
 141 MATLAB). The variability in the parameters among the field-plots can be visualized by means of a heat  
 142 map (see Fig 4). The effect of various treatments of the crop can be evaluated by analyzing the  
 143 variability among the  $A$ ,  $B$  and  $C$  parameters inferred from the crop heights.



144  
 145 **Figure 4** Visualization of the parameters of the sigmoid growth model for individual field-plots. Parameter  $A$  (left panel)  
 146 corresponds to the maximum possible height of the crop. Parameter  $B$  (middle panel) captures the “growth velocity” because  
 147 it corresponds to the slope of the sigmoid curve. Parameter  $C$  (right panel) is the “offset” which captures the left-right shift  
 148 of the sigmoid. Parameters are shown for blocks of field-plots 1, 2 and 3 as indicated by the red numbers in the top row. The  
 149 left column of numbers stands for the ID of the variant, the right column shows the numerical value of the respective  
 150 parameter of the sigmoid model. The parameter values are color coded. Observe the spatially correlated variability in the  
 151 parameters.

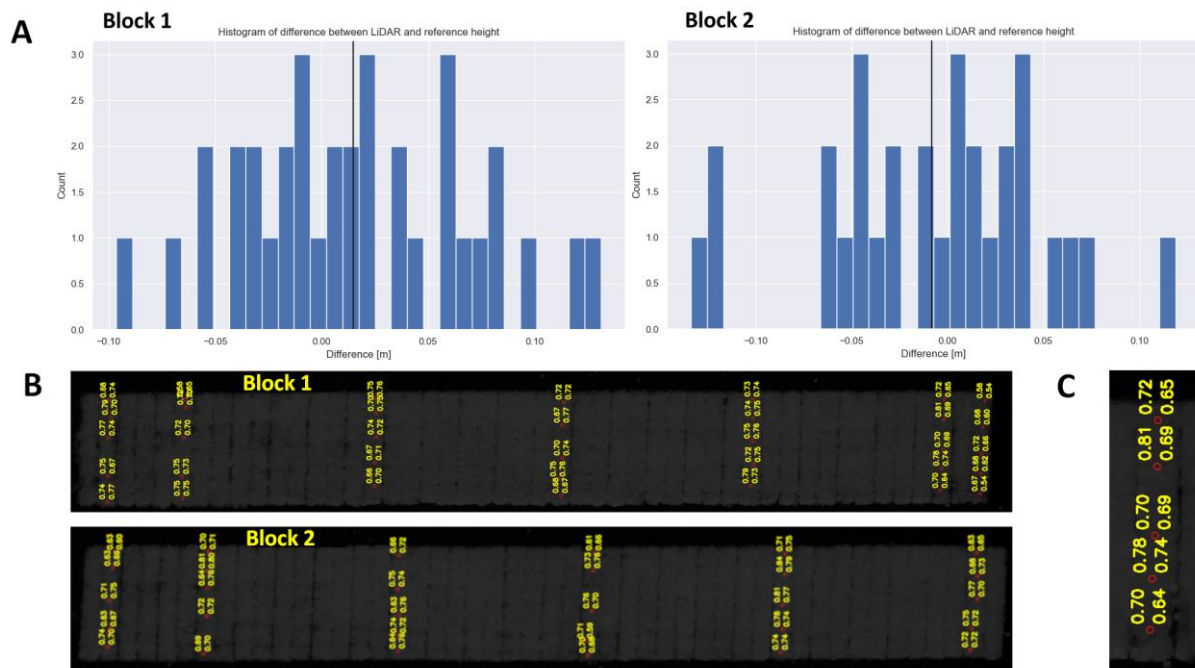
152

## 153 **RESULTS AND DISCUSSION**

154 Data for software testing and optimization were acquired using UAV LiDAR system (Ricopter VUX-SYS,  
155 Riegl GmbH, Austria) using same parameters as described previously (Polák et al., 2021). Eight flights  
156 from March to June were performed to scan an array of barley field-plots organized into three  
157 experimental blocks (48 variants per each block). The flight altitude was set to 20 m AGL, horizontal  
158 speed of flight 4 m/s, scanning line distance 9 m, calculated side overlap (77%, 31 m). The LiDAR sensor  
159 was running at the maximum laser pulse rate (550 kHz). LiDAR scans were processed as described  
160 previously to point-cloud files in the “las” format. These files were processed by our software to  
161 segment point-cloud derived crop height model (CHM) and analyze the crop height at individual field-  
162 plots.

### 163 **Manual validation in selected field-plots**

164 To validate the software and assess the UAV LiDAR scanning accuracy, we performed manual  
165 measurement using geodetic GPS and a ruler to measure the crop height. These measurements were  
166 performed the same day as the UAV LiDAR scanning and covered 6 and 7 field-plots homogeneously  
167 distributed across blocks 1 and 2. We performed validation of the crop height measurement in two  
168 blocks 1 and 2 by manually measuring the crop height at 5 points within each field-plot (see Figure 5).  
169 Our validation showed that the Root Mean Square Deviation (RMSD) of the software-computed crop  
170 height from the manual measurement was 5.7 cm (0.057 m) for both blocks together. The error  
171 distribution for each individual block is depicted in Figure 5. This is better than the results reached  
172 with the previous software that was validated in wheat field-plots (Polák et al., 2021). The manual  
173 measurements are based on the median of 5 values, whereas the LiDAR data reflect the height of the  
174 entire plot.



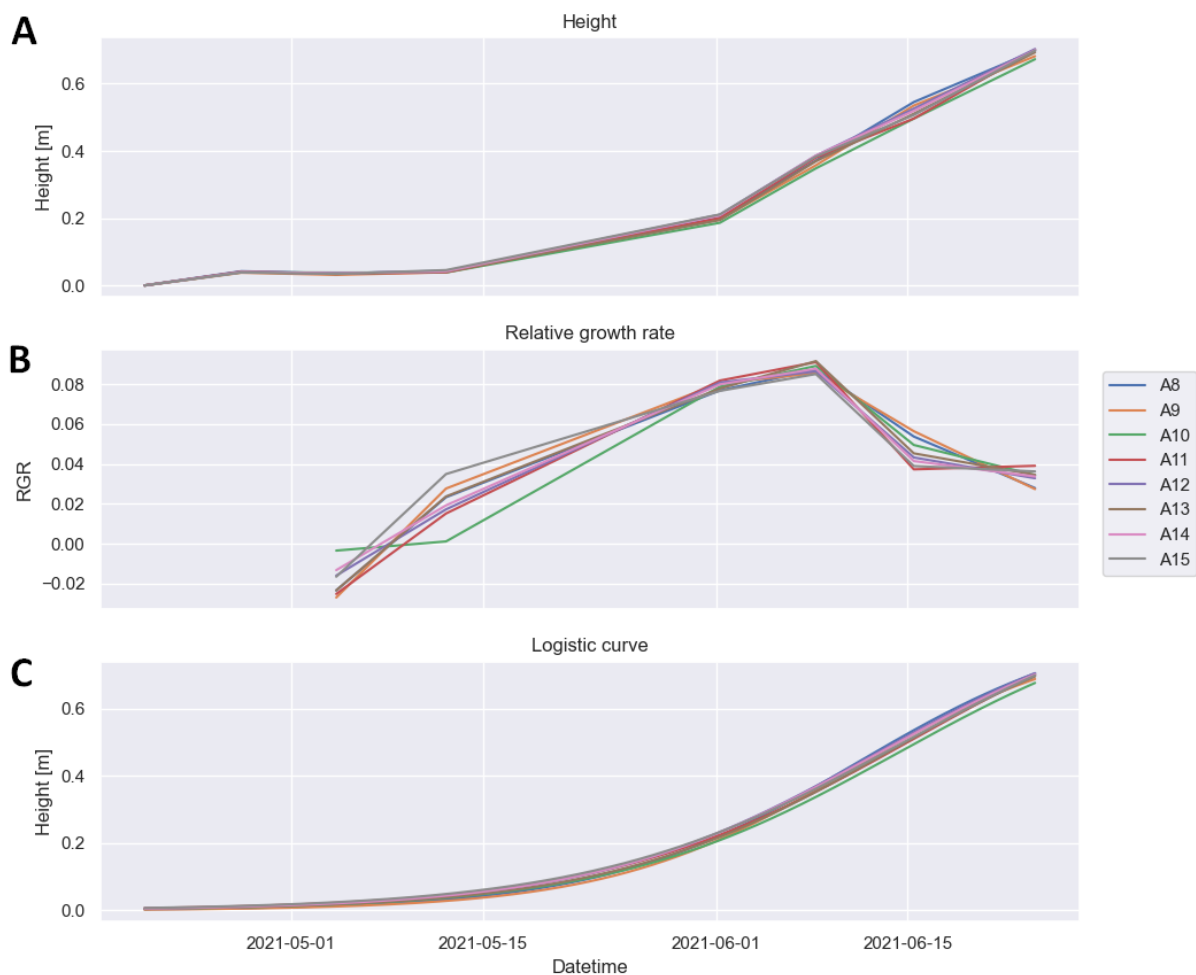
175

176 **Figure 5** Manual validation of the ALFA software crop height assessment. A) Distribution of the difference between the  
 177 software-computed crop height and the manual measurement. Blocks 1 and 2 are shown separately. B) Visualization of the  
 178 field-plots that were included in the validation, identification of blocks 1 and 2. C) A detailed view of a selected field-plot  
 179 showing the points of validation. The values in the right column show the software-computed crop height and the particular  
 180 point. The values in the left column represent the manual measurement.

181 **Dynamical analysis of crop height**

182 Measurement of crop height at a single time-point may not be sufficient in many cases. Plant growth  
 183 is a dynamic process which is highly non-linear (Cao and Moss, 1989). To assess crop growth, we  
 184 measure the crop height at multiple time points during the vegetative developmental phase. In our  
 185 case, we performed 7 UAV scanning flights over 3 experimental blocks with a total of 144 barley field-  
 186 plots. Seven scanning flights were performed between April and June 2021. Scanning was performed  
 187 in automatic flight mode at 20 m AGL height. After necessary pre-processing steps, the point-cloud  
 188 files were processed by our software (see Implementation). Multiple time-point measurements then  
 189 allow to visualize growth in various ways: A simple bar graph of crop height at particular time-points,  
 190 relative growth rates based on crop height data, or parameters of the sigmoid model fitted to the  
 191 growth curve. Plotting crop height (Fig 6A) is the most straight-forward way but it does not allow for  
 192 easy comparison of growth dynamics in individual field-plots. This is better visualized by a sigmoid fit  
 193 of the growth curve (Fig 6C). It shows the overall dynamics of vegetative growth for each plot, but

194 information about plant performance from individual time-points is hidden. On the contrary, RGR (Fig.  
195 6B) shows the growth rate in particular time-points and helps to understand the overall dynamics of  
196 plant growth. The three parameters of the sigmoid (A, B, and C, see section Implementation above)  
197 can also be visualized separately by means of a heat map (see Fig. 4).



198  
199 **Figure 6** Barley growth during vegetation season in selected representative field-plots. For the individual field-plots, the figure  
200 shows the evolution of the crop height (A), RGR (B) and logistic (sigmoid) curves (C).

201 To test our new software, we evaluated crop growth in 3 blocks, in the total of 144 field-plots. All of  
202 the plots contained the same genotype (cv. Francin), sown in a place where we previously observed  
203 very heterogeneous growth characteristics in cereals. For this reason, we decided to visualize the  
204 growth heterogeneity using a precise measurement of plant growth dynamics. Important differences  
205 in growth dynamics are obvious from the RGR and growth curve parameters (Fig 6B, C). The  
206 heterogeneity is particularly visible in the heat map (Fig 4) of the sigmoid growth model parameters.

207 The heat map shows “patterns” of spatially correlated growth differences. It is known that barley is  
208 sensitive to different soil compaction that significantly affects root and shoot growth (Mulholland et  
209 al., 1996). Since chemical analysis did not reveal any important variability in chemical and nutritional  
210 composition of soil (data not shown), we hypothesize that the physical properties of the soil play the  
211 key role.

## 212 **CONCLUSION**

213 The aim of the software development was to design and optimize an algorithm capable of fast  
214 extraction of crop height from point-clouds obtained by UAV LiDAR scanning. The ALFA software  
215 (available freely for non-commercial use here: <https://github.com/frycaktadeas/alfa>) uses point-cloud  
216 data, converts them into a digital image, and extracts the trait of interest. The entire analysis of 144  
217 field plots (1.2 x 9 meters each) measured at 7 time points takes about 3 minutes at a standard PC. The  
218 RMSD difference between the ALFA software computed crop height (from UAV LiDAR data) and a  
219 manual measurement (by a ruler) was 5.7 cm. Three different ways of expressing the plant growth  
220 dynamics are introduced to allow for understanding the plant growth dynamics and plant reactions to  
221 environmental changes. For the future, we plan to add a statistical toolbox to the ALFA software. The  
222 toolbox will assess the plant growth dynamic by means of hierarchical Bayesian model that correctly  
223 accounts for the spatially correlation of the growth dynamics. In this way, the true effects of treatment  
224 can be extracted from the inherently correlated growth data.

## 225 **Availability of data and materials**

226 Software tool is freely accessible here: <https://github.com/frycaktadeas/alfa>

227 The datasets analyzed during the current study are available from the corresponding author on  
228 reasonable request.

## 229 **Competing interests**

230 The authors have declared that no competing interests exist.

231 **Funding**

232 The work was supported by the ERDF project "Plants as a tool for sustainable global development"  
233 (No. CZ.02.1.01/0.0/0.0/16\_019/0000827).

234 **REFERENCES**

- 235 Brede, B., Lau, A., Bartholomeus, H.M., Kooistra, L., 2017. Comparing RIEGL RiCOPTER UAV LiDAR  
236 derived canopy height and DBH with terrestrial LiDAR. *Sensors (Switzerland)* 17.  
237 <https://doi.org/10.3390/s17102371>
- 238 Cao, W., Moss, D.N., 1989. Temperature Effect on Leaf Emergence and Phyllochron in Wheat and  
239 Barley. *Crop Sci.* 29, 1018–1021.  
240 <https://doi.org/10.2135/CROPSCI1989.0011183X002900040038X>
- 241 French, A.N., Gore, M.A., Thompson, A., 2016. Cotton phenotyping with lidar from a track-mounted  
242 platform, in: *Autonomous Air and Ground Sensing Systems for Agricultural Optimization and*  
243 *Phenotyping. Conference on Autonomous Air and Ground Sensing Systems for Agricultural*  
244 *Optimization and Phenotyping*, p. 98660B. <https://doi.org/10.1117/12.2224423>
- 245 GAO, Min, et al. Individual maize location and height estimation in field from UAV-borne LiDAR and  
246 RGB images. *Remote Sensing*, 2022, 14.10: 2292.
- 247 GRANSHAW, Stuart I. Photogrammetric terminology. *The Photogrammetric Record*, 2016, 31.154:  
248 210-252.
- 249 Hoffmann, W.A., Poorter, H., n.d. Avoiding Bias in Calculations of Relative Growth Rate.  
250 <https://doi.org/10.1093/aob/mcf140>
- 251 Holman, F.H., Riche, A.B., Michalski, A., Castle, M., Wooster, M.J., Hawkesford, M.J., 2016. High  
252 throughput field phenotyping of wheat plant height and growth rate in field plot trials using  
253 UAV based remote sensing. *Remote Sens.* 8. <https://doi.org/10.3390/rs8121031>
- 254 HÜTT, Christoph, et al. UAV LiDAR Metrics for Monitoring Crop Height, Biomass and Nitrogen Uptake:  
255 A Case Study on a Winter Wheat Field Trial. *PFG—Journal of Photogrammetry, Remote Sensing*  
256 *and Geoinformation Science*, 2022, 1-12.
- 257 Iglhaut, J., Cabo, C., Puliti, S., Piermattei, L., O’connor, J., Rosette, J., Uk, A.A., Gutiérrez Quirós, G.,  
258 2019. Structure from Motion Photogrammetry in Forestry: a Review.  
259 <https://doi.org/10.1007/s40725-019-00094-3>
- 260 JIN, Shichao, et al. Deep learning: individual maize segmentation from terrestrial lidar data using  
261 faster R-CNN and regional growth algorithms. *Frontiers in plant science*, 2018, 9: 866.
- 262 KOCH, Barbara; HEYDER, Ursula; WEINACKER, Holger. Detection of individual tree crowns in airborne  
263 lidar data. *Photogrammetric Engineering & Remote Sensing*, 2006, 72.4: 357-363.
- 264 LI, Wenkai, et al. A new method for segmenting individual trees from the lidar point cloud.  
265 *Photogrammetric Engineering and Remote Sensing*, 2012, 78.1: 75-84.

266 LIU, Kuan; DONG, Xiaoya; QIU, Baijing. Analysis of cotton height spatial variability based on UAV-  
267 LiDAR. *International Journal of Precision Agricultural Aviation*, 2020, 3.3.

268 Malambo, L., Popescu, S.C., Murray, S.C., Putman, E., Pugh, N.A., Horne, D.W., Richardson, G.,  
269 Sheridan, R., Rooney, W.L., Avant, R., Vidrine, M., McCutchen, B., Baltensperger, D., Bishop, M.,  
270 2018. Multitemporal field-based plant height estimation using 3D point clouds generated from  
271 small unmanned aerial systems high-resolution imagery. *Int. J. Appl. Earth Obs. Geoinf.* 64, 31–  
272 42. <https://doi.org/10.1016/j.jag.2017.08.014>

273 MONTZKA, Carsten, et al. Sensitivity of LiDAR Parameters to Aboveground Biomass in Winter Spelt.  
274 *Drones*, 2023, 7.2: 121.

275 Mulholland, B.J., Black, C.R., Taylor, I.B., Roberts, J. a, Lenton, J.R., 1996. Effect of soil compaction on  
276 barley (*Hordeum vulgare* L) growth .1. possible role for ABA as a root-sourced chemical signal. *J.*  
277 *Exp. Bot.* 47, 539–549.

278 OpenCV, L., 2008. Computer vision with the OpenCV library. Gary Bradski, Adrian Kaehler 1–15.

279 Polák, M., Mirijovský, J., Hernández, A.E., Špíšek, Z., Koprna, R., Humplík, J.F., 2021. Innovative uav  
280 lidar generated point-cloud processing algorithm in python for unsupervised detection and  
281 analysis of agricultural field-plots. *Remote Sens.* 13. <https://doi.org/10.3390/rs13163169>

282 TEN HARKEL, Jelle; BARTHOLOMEUS, Harm; KOOISTRA, Lammert. Biomass and crop height  
283 estimation of different crops using UAV-based LiDAR. *Remote Sensing*, 2019, 12.1: 17.

284 TJØRVE, Even. Shapes and functions of species–area curves: a review of possible models. *Journal of*  
285 *Biogeography*, 2003, 30.6: 827-835.

286 WANG, Han, et al. Maize Ear Height and Ear–Plant Height Ratio Estimation with LiDAR Data and  
287 Vertical Leaf Area Profile. *Remote Sensing*, 2023, 15.4: 964.

288 WANG, Yunsheng, et al. Lidar point cloud based fully automatic 3D single tree modelling in forest and  
289 evaluations of the procedure. *Int. Arch. Photogramm. Remote Sens. Spat. Inf. Sci.* 2008, 37.Part  
290 B6b: 45-51.

291 Zhu, Y., Sun, G., Ding, G., Zhou, Jie, Wen, M., Jin, S., Zhao, Q., Colmer, J., Ding, Y., Ober, E.S., Zhou, Ji,  
292 2021. Large-scale field phenotyping using backpack LiDAR and CropQuant-3D to measure  
293 structural variation in wheat. *Plant Physiol.* 187, 716–738.  
294 <https://doi.org/10.1093/plphys/kiab324>

295